J. Am. Chem. Soc. 1983, 105, 3381-3387

Cryochemical Studies. 6. ESR Studies of the Reaction of Group 1B Metal Atoms with Arenes at 77 K in a Rotating Cryostat[1]

A. J. Buck,[†] B. Mile,*[†] and J. A. Howard*[‡]

Contribution from the Department of Chemistry and Biochemistry, Liverpool Polytechnic,
Byrom Street, Liverpool, England L3 3AF, and Division of Chemistry,
National Research Council of Canada, Ottawa, Canada K1A 0R9. *Received June 8, 1982*

Abstract: Group 1B metal atoms have been deposited into "inert" hydrocarbon and reactive arene matrices at 77 K in a rotating cryostat and their electron spin resonance spectra have been examined. The spectra show that the metal atoms Cu, Ag, and Au(M) are trapped in adamantane and cyclohexane at 77 K with less perturbation of the singly occupied atomic orbital than atoms trapped in rare gas matrices. In the case of benzene, the spectra indicate formation of metal atom–monoligand complexes, $M(C_6H_6)$. $Cu(C_6H_6)$ has an anisotropic **g** tensor, an almost isotropic **A** tensor and ~70% unpaired 4s spin population in the singly occupied molecular orbital (SOMO). $Au(C_6H_6)$ and $Ag(C_6H_6)$ have axially symmetric and isotropic parameters, respectively. The SOMO for the Ag and Au complexes have ~95% unpaired s spin population. Substitution onto the benzene of electron withdrawing and donating substituents leads to complete destabilization of the copper complex and some loss of stability of the silver and gold complexes with little change in their ESR parameters. The difference between $Cu(C_6H_6)$ and $Ag(C_6H_6)$ (and $Au(C_6H_6)$) may arise from the higher energy level of the Cu 3d orbitals relative to the benzene orbitals. Bonding in $Cu(C_6H_6)$ may involve interaction between 3d and 4p orbitals of the correct symmetry with the upper $1e_{1g}$ benzene orbitals and leads to a SOMO having metal 4p and 3d as well as 4s character. In $Ag(C_6H_6)$ and $Au(C_6H_6)$ bonding may involve interaction between 4d, 5p, 5d, and 6p orbitals with the lower $1a_{2u}$ benzene orbitals leading to an almost pure metal 5s and 6s SOMO. In most cases ESR spectra arising from metal atom clusters and microcrystallites are also observed.

Introduction

Cryochemical techniques are now being increasingly used to make a range of new stable organometallic compounds.[2-6] In addition, the preparation and study of metal atom clusters and unstable metal organic complexes at 77 K is directly relevant to an understanding of heterogeneous catalysis and may also provide the basis for a new method for preparing highly active catalysts.[7-9] However, the mechanisms of formation and structures of most of these labile low-temperature complexes still remain obscure. Kasai, McLeod and Watanabe[10] recently reported a thorough investigation of the electron spin resonance spectra (ESR) of the complexes of Cu and Ag with acetylene and ethylene and have provided convincing evidence for the formation of both monoligand and biligand complexes. The electronic and vibrational spectra of Cu, Ag, and Au complexes with ethylene and acetylene have also been observed and assigned by Ozin.[11,12] The SCF-Xα-SW method has recently been applied by MacIntosh, Ozin, and Messmer[12] to elucidate the bonding in these complexes. They find that the major bonding interaction is of the Dewar–Chatt–Duncanson type[13,14] with a donation of charge from the π bonds of the organic moiety to the metal d orbitals. There is little of the back donation from the metal to the π^* antibonding orbitals suggested by Kasai, McLeod, and Watanabe.[10]

Here we report the results of our studies of the reaction of group 1B metal atoms with a range of arenes, using a rotating cryostat.[15,16] Apart from the pioneering work on group 1B atoms by Zhitnikov and co-workers[17-24] little is known about these systems other than for the complex of Ag with toluene produced by γ-irradiated of frozen solutions of $AgClO_4$/8-crown-6-ether in toluene.[25]

Experimental Section

Materials. Benzene, substituted benzenes, perfluorobenzene, cyclohexane, and adamantane were thoroughly dried over molecular sieve 3A, distilled, and degassed before use. Perdeuteriobenzene and benzene enriched to 90% in ^{13}C were purchased from Merck, Sharpe and Dohme, Canada Ltd. Copper, silver, and gold sheets and powder (purity >99.99%) were purchased from Goodfellow Metals (U.K.) and were also gifts from Dr. C. M. Hurd (N.R.C. Ottawa). CuO enriched to 99.89% in ^{63}Cu and Ag enriched to 99.9% in ^{107}Ag were obtained from Oak Ridge National Laboratory, TN. ^{63}CuO was reduced to ^{63}Cu with hydrogen at 500 °C.

Rotating Cryostat and Furnace. Rotating cryostats similar to that described by Bennett, Mile, Thomas, and Ward[15,16] were used to deposit the metal atoms onto frozen layers of the organic reactants at 77 K. One of the plugs fitting into the outer housing of the cryostat was modified

---

[‡] National Research Council.
[†] Liverpool Polytechnic.

(1) Issued as NRCC 21148. For part 5, see: Howard, J. A.; Sutcliffe, R.; Mile, B. *J. Am. Chem. Soc.* **1983**, *105*, 1394–1395.

(2) Timms, P. L. *Angew. Chem. Int. Ed. Engl.* **1975**, *14*, 273–374.

(3) "Cryochemistry;" Moskovits, M.; Ozin, G. A., Ed.; Wiley: New York, 1976.

(4) Blackborow, J. R.; Young, D. "Metal Vapour Synthesis in Organometallic Chemistry; Reactivity and Structure, Concepts in Organic Chemistry"; Vol. 9, Springer-Verlag: Berlin, 1979.

(5) Klabunde, K. J. "Chemistry of Free atoms and Particles"; Academic Press: New York, 1980.

(6) Faraday Symposia of the Chemical Society, No. 14, 1980.

(7) Klabunde, K. J.; Ralston, D.; Zoellner, R.; Hattori, H.; Tanaka, Y. *J. Catal.* **1978**, *55*, 213–227.

(8) Candlin, J. P. U.S. Patent 48 406, 1975.

(9) Moskovits, M. *Acc. Chem. Res.* **1979**, *12*, 229–236.

(10) Kasai, P. H.; McLeod, D., Jr.; Watanabe, T. *J. Am. Chem. Soc.* **1980**, *102*, 179–190.

(11) Ozin, G. A. *Acc. Chem. Res.* **1977**, *10*, 21–26, and references cited therein.

(12) (a) McIntosh, D. F.; Ozin, G. A.; Messmer, R. P. *Inorg. Chem.* **1980** *19*, 3321–3327. (b) Ozin, G. A.; McIntosh, D. F.; Power, W. J.; Messmer, R. P. *Ibid.* **1981**, *20*, 1782–1792.

(13) Dewar, M. J. S. *Bull. Soc. Chim. Fr.* **1951**, *18*, C71–79.

(14) Chatt, J.; Duncanson, L. A. *J. Chem. Soc.* **1953**, 2939–2947.

(15) Bennett, J. E., Thomas, A. *Proc. R. Soc. London, Ser. A* **1964**, *280*, 123–138.

(16) Bennett, J. E.; Mile, B.; Thomas, A.; Ward, B. *Adv. Phys. Org. Chem.* **1970**, *8*, 1.

(17) Zhitnikov, R. A.; Kolesnikov, N. V.; Kozyakov, V. I. *Zh. Eksp. Theor. Fiz.* **1962**, *43*, 1186–1196; *Sov. Phys. JEPT* **1963**, *16*, 839–846.

(18) Zhitnikov, R. A.; Kolesnikov, N. V.; Kozyakov, V. I. *Zh. Eksp. Theor. Fiz.* **1963**, *44*, 1204–1210; *Sov. Phys. JEPT* **1963**, *17*, 815–819.

(19) Zhitnikov, R. A.; Kolesnikov, N. V. *Zh. Eksp. Theor. Fiz.* **1964**, *46*, 89–98; *Sov. Phys. JEPT* **1964**, *19*, 65–71.

(20) Zhitnikov, R. A.; Kolesnikov, N. V. *Fiz. Tverd. Tela* **1964**, *6*, 3307–3316; *Sov. Phys. Solid* **1965**, *6*, 2645–2651.

(21) Zhitnikov, R. A.; Kolesnikov, N. V. *Fiz. Tverd. Tela* **1965**, *7*, 1263–1264; *Sov. Phys. Solid State* **1965**, *7*, 1021–1022.

(22) Zhitnikov, R. A.; Kolesnikov, N. V. *Fiz. Tverd. Tela* **1965**, *7*, 1710–1716; *Sov. Phys. Solid State* **1965**, *7*, 1382–1387.

(23) Zhitnikov, R. A.; Kolesnikov, N. V. *Fiz. Tverd. Tela* **1967**, *9*, 162–166; *Sov. Phys. Solid State* **1967**, *9*, 121–124.

(24) Zhitnikov, R. A.; Mel'nikov, M. I.; Orbeli, A. L. *Zh. Strukt. Khim.* **1968**, *9*, 616–620.

(25) Jerzierska, J.; Raynor, J. B. *J. Chem. Soc., Dalton Trans.* **1981**, 56–60.

0002-7863/83/1505-3381$01.50/0 Published 1983 by the American Chemical Society

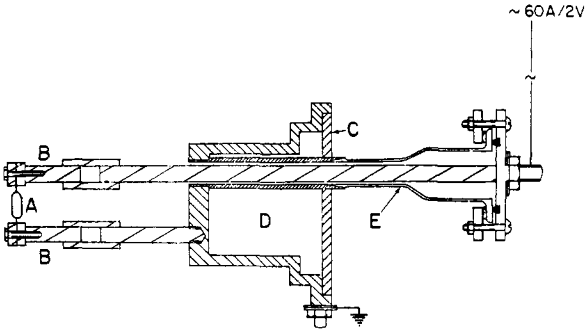

Figure 1. High-temperature furnace assembly for use with the rotating cryostat: (A) molybdenum pouch; (B) molybdenum electrodes; (C) brass plug; (D) water coolant circulated through this section; and (E) glass flange and sleeve.

to hold the resistively heated furnace assembly shown in Figure 1. The plug itself and outer connecting rods were made of stainless steel and were water cooled. The hot furnace components were made of molybdenum rod and sheet. The metal to be evaporated as atoms was placed in sheet or powder form in a molybdenum pouch constructed from 0.001-in. sheet having a vertical slit to direct the metal vapor onto the cold surface of the rotating drum about 4 mm away. An alumina liner was incorporated into the pouch for some experiments to minimize alloying. The hanging drop method was also used: the metal was vaporized from a drop suspended on a heated V-shaped tungsten rod of 2 mm diameter clamped between molybdenum electrodes. Similar ESR spectra were obtained from the three types of furnace although the relative intensities of the different paramagnetic species depended on the amount of metal deposited. A step-down transformer provided currents of ~60 A at ~2 V to heat the pouch or hanging drop. Temperatures (usually ~1300 °C) were measured through an adjacent viewing port using a Leeds-Northrop optical pyrometer or a Goulton infrared pyrometer. The furnace could be heated to ~2300 °C without any deleterious effects.

Experimental Procedure. In a typical experiment the vapors of the organic substrate and metal were condensed *separately* onto the cold surface of the stainless steel drum containing liquid nitrogen and spinning at 2400 rpm in a high vacuum ($>10^{-5}$ torr). The cryostat was usually run for ~0.5 h, and in that time 2–10 mg of metal and ~1 g of organic matrix were deposited. The metal and substrate formed interleaving spirals in which the transient species were trapped at 77 K. Deposits were removed from the surface of the drum at this temperature and transferred to a tube suitable for ESR investigation. The unique feature of the technique is the spatial and temporal separation of the metal and organic substrate so that the metal atoms react with and are trapped on a cold surface rather than in the "slush" phase encountered in many traditional co-condensation methods.

ESR Measurements. ESR spectra were recorded at 77 K on a Varian V-4502 spectrometer with Field-dial regulation of the magnetic field and a Varian E-12 spectrometer. The microwave frequency was measured with a Systron-Donner Model 6057 frequency counter and the magnetic field with a Cyclotron Model 5300 NMR gaussmeter. The hyperfine values are correct to ±2 G and the g values to ±0.0002. All ESR parameters were calculated from exact solutions of the spin Hamiltonians using computer programs made available by Drs. J. R. Morton and K. F. Preston (NRC, Ottawa). Spectra were recorded at higher temperatures by use of a variable temperature accessory.

Results and Discussion

Inert Matrices. Cu + Adamantane. The deposit from Cu atoms ($I = {}^3/_2$) in adamantane gave an ESR spectrum at 77 K which consisted of four almost isotropic lines at 1284.9, 1771.13, 5559.01, and 5687.9 G and an anisotropic multiplet centered at ~3200 G (ν = 9034 MHz). The two low-field lines were more anisotropic than the high-field lines and were assigned to the NMR transition $M_s = -{}^1/_2$, $M_I = -{}^3/_2 \leftrightarrow -{}^1/_2$ from the two isotopes of copper.[26] The two high-field lines can be assigned to the ESR transition $\Delta M_S = \pm 1$ $M_I = -{}^3/_2$ from ^{63}Cu and ^{65}Cu atoms. The three other ESR transitions, $M_I = -{}^1/_2, +{}^1/_2$, and $+{}^3/_2$, were not detected because the spectrometer frequency was less than the zero-field splitting, $(I + {}^1/_2)g\beta A$.[26,27] The ESR spectrum of ^{63}Cu atoms in adamantane is shown in Figure 2a. We can conclude from this spectrum that there is one major trapping site for Cu atoms in this matrix, and the near isotropic shape of the lines indicates that the trapping site has almost cubic symmetry. An exact solution of an isotropic spin Hamiltonian[26,27] gave the following parameters for Cu atoms trapped in adamantane: A_{65} = 2196.2 G, g = 2.0016; A_{63} = 2050.5 G, g = 2.0016.

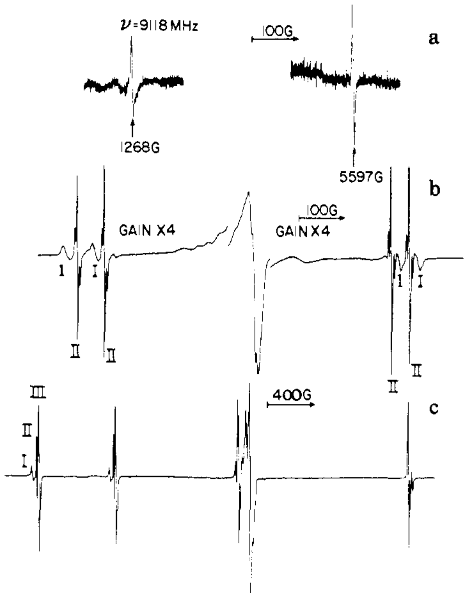

Figure 2. ESR spectra of adamantane containing group 1B metal atoms at 77 K: (a) ^{63}Cu; (b) ^{107}Ag and ^{109}Ag; (c) ^{197}Au.

The ratio A_{65}/A_{63} of 1.0712 is identical with the ratio of the nuclear magnetic moments for copper 65 and 63. The ^{63}Cu hyperfine interaction (HFI) in adamantane is slightly smaller than the value found in the gas phase (2093 G) from atom beam experiments, $(A_0 - A_{\mathrm{Cu}})/A_0 = 2.1 \times 10^{-2}$, and is significantly smaller than the HFI obtained in inert gases. For example, A_{63} has a value of 2112 G in Xe and a value of 2198 G in Ar.[26] Furthermore, the g factor in adamantane is much closer to the free spin value than the values obtained in inert-gas matrices (g < 1.999). The A_{Cu} and g values in adamantane are quite close to those reported by Zhitnikov and Kolesnikov[20] for Cu atoms in undecane (A_{63} = 2122 G, g = 2.0028).

The nearest neighbor spacing in adamantane is about 5 Å, significantly larger than in the inert gas matrices (e.g., argon, 3.83 Å; xenon, 4.41 Å). This may be the reason for the proximity of the g factor to the free spin value and the slight reduction in the HFI compared with the gas phase value. It would, therefore, appear that the copper atom in adamantane is either suffering very little perturbation by the matrix or there is a cancellation of the three factors of overlap, replusion, and attractive van der Waals interaction. These are thought by Adrian[28] and Jen and co-workers[29] to be important in affecting the ESR spectra of trapped atoms. The parameters of atoms trapped in adamantane appear to be the most suitable as the basic comparison parameters for atoms trapped in a matrix and undergoing little interaction with matrix molecules. We have used them in this way in the present work.

The multiplet centered at ~3200 G appeared to be an axially symmetric copper species with an anisotropic hyperfine interaction and an almost isotropic g tensor. A good simulation of this spectrum was obtained using the ESR parameters g = 2.0024, $A_\parallel$ = 46 G $A_\perp$ = 10 G, indicating quite a small copper hyperfine interaction. This spectrum has not yet been assigned.

Ag + Adamantane. The ESR spectrum produced by Ag atoms in adamantane, shown in Figure 2b, has three distinct features:

---

[26] Kasai, P. H.; McLeod, D., Jr. *J. Chem. Phys.* **1971**, *55*, 1566–1575.

[27] Boate, A. R.; Morton, J. R.; Preston, K. F. *J. Magn. Res.* **1976**, *24*, 259–268.

[28] Adrian, F. J. *J. Chem. Phys.* **1960**, *32*, 972–981.

[29] Jen, C. K.; Bowers, V. A.; Cochran, E. L.; Foner, S. N. *Phys. Rev.* **1962**, *126*, 1749–1757.

(i) two sets of sharp isotropic lines showing triplet structure at 2838.7, 2895.6, 3501, and 3538.3 G; (ii) two sets of weaker and broader asymmetric lines at 2820, 2876.6 3515, and 3552.4 G; and (iii) a broad anisotropic feature centered at ~3200 G showing some hyperfine interaction.

Considering the first two features, the zero-field splitting for silver atoms is considerably smaller than the microwave frequency used (9039.5 MHz) and hence the two ESR transitions, $M_I = -{}^1/_2$ and $M_I = +{}^1/_2$ of the two silver isotopes can be observed. Unlike the case of copper atoms, there are two major trapping sites for silver atoms in adamantane, one leading to sharp isotropic lines (site II) and the other to broader more asymmetric lines associated with a larger HFI (site I). Similar subtle difference in the number of different trapping sites for group 1B metal atoms have been observed by Kasai and McLeod[26] for inert gas matrices. They attribute the broad and sharp features to trapping in amorphous and crystalline regions, respectively.

The following parameters were obtained for the two isotopes of silver: site I, A_{109} = 727.5 G, g = 2.0023; A_{107} = 632.2 G, g = 2.0014; site II, A_{109} = 691.6 G, g = 2.0020; A_{107} = 600.1 G, g = 2.0018. The g factors for the two sets are close to the free spin value, in contrast to the negative shift of 0.0023 obtained for silver atoms in rare gas matrices.[26] The A_{109}/A_{107} ratio of 1.1511 is close to the ratio of the magnetic moments (1.1496) and there is good agreement with the A_{Ag} and g values reported by Zhitnikov and Kolesnikov.[19]

The silver HFI for site I is slightly larger than that found in the gas phase (611 G), giving $(A_0 - A_{\mathrm{Ag}})/A_0 = -0.347 \times 10^{-2}$. It is comparable to that found in rare gas matrices. The HFI for site II is slightly smaller than the gas phase value with $(A_0 - A_{\mathrm{Ag}})/A_0 = 1.8 \times 10^{-2}$. It is likely that in site I the atoms are associated with a range of trapping sites in highly amorphous regions of the matrix and that the broadening is due to a multiplicity of trapping sites. It appears that there is a preponderance of the overlap and repulsive interactions which lead to an increase in spin density at the silver nucleus; a similar increase was observed for Cu atoms trapped in neon.[26] We believe that the parameters for site II are those that should be used for comparison purposes.

We attribute the triplet feature associated with site II to forbidden proton "spin-flip" satellites.[30-34] The most direct proof for this assignment is the marked decrease in the ratio of the intensity of the central line to that of the outer lines with an increase in microwave power, the ratio dropping from ~9.1 at 0.5 mW to ~2.9 at 5 mW. The separation of the satellite lines is also consistent with them arising from proton spin flips. The satellites of the high-field line at 3501 G are separated by ~5.5 G from the main line which corresponds to a spacing of ~15.3 MHz at the microwave frequency used (9039.5 MHz). This is close to the expected proton NMR frequency of 14.9 MHz at 3501 G. The intensity ratio and separation of the satellite lines from the main line can be used to estimate the distance of the free electron from the protons that are flipping. The estimates will not be of high accuracy because of the inverse sixth power relationship between the distance and the measured parameters.[30,33] The distance of ~2.6 Å obtained is acceptable in view of the next nearest neighbor spacing of ~5 Å for adamantane and the known van der Waals radius of 2.35 Å for silver atoms.

The anisotropic feature centered at 3200 G is a composite spectrum from silver aggregates and an anisotropoic conduction electron ESR spectrum arising from microcrystalline particles of silver.[35] These features provide valuable information about aggregate and particle size and will be considered fully in a later publication.

Table I. ESR Parameters for Group 1B Metal Atoms Trapped in Inert Hydrocarbon Matrices at 77 K

metal (M)	matrix	g factor	A_M/G
^{65}Cu	adamantane	2.0016	2196.2
^{63}Cu	adamantane	2.0016	2050.5
^{65}Cu	cyclohexane	2.0020	2200.0
^{63}Cu	cyclohexane	2.0021	2054.0
^{65}Cu	gas phase	2.0023	2242.5
^{63}Cu	gas phase	2.0023	2093.5
^{109}Ag	adamantane site I	2.0023	727.5
	adamantane site II	2.0020	691.6
^{107}Ag	adamantane site I	2.0014	632.2
	adamantane site II	2.0018	600.1
^{109}Ag	cyclohexane	2.0020	709.5
^{107}Ag	cyclohexane	2.0021	614.9
^{109}Ag	gas phase	2.0023	705.4
^{107}Ag	gas phase	2.0023	611.0
^{197}Au	adamantane site I	2.0017	1046.4
	adamantane site II	2.0022	1028.0
	adamantane site III	2.0016	1018.4
^{197}Au	cyclohexane site I	2.0038	1069.0
	cyclohexane site II	2.0030	1044.0
	cyclohexane site III	2.0023	1030.0
^{197}Au	gas phase	2.0023	1088.2

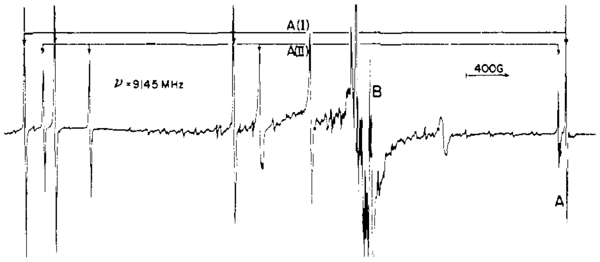

Figure 3. ESR spectra of benzene containing ^{63}Cu atoms at 77 K.

Au + Adamantane. The ESR spectrum of gold, ^{197}Au ($I = {}^3/_2$) atoms in adamantane, shown in Figure 2c, consists of three almost isotropic quartets with large gold HFI and an anisotropic multiplet in the free-spin region. No proton spin-flip lines are observed probably because the Au lines are almost twice as wide as the Ag lines. Clearly there are three major magnetically different trapping sites for gold atoms in adamantane with the following ESR parameters: site I, A_{Au} = 1046.4 G; g = 2.0017; site II, A_{Au} = 1028 G; g = 2.0022; site III, A_{Au} = 1018.4 G; g = 2.0016.

The g factors are again very close to the free-spin value but in this case the HFI for all three sites are slightly less than that for Au atoms in the gas phase, e.g., $A_0 - A_{\mathrm{Au}}/A_0 = 6.4 \times 10^{-2}$ for site III. Zhitnikov and Kolesnikov observed only one trapping site for gold atoms in undecane with A and g values of 1055 G and 2.0042.[19] The parameters for site III will be used as a reference for unbound Au atoms in the solid state.

The anisotropic feature centered at about 3200 G is attributed to Au aggregates and microcrystallites.

Cu, Ag, and Au in Cyclohexane. The ESR spectra of group 1B atoms trapped in cyclohexane at 77 K were very similar to those in adamantane except that only one trapping site was observed for Ag. The atoms decayed much more rapidly than in adamantane and were not observed at all in some experiments. To our knowledge, this is the first observation of atoms trapped in a low molecular weight saturated hydrocarbon at 77 K. Spin-flip satellites were again seen in the case of silver atoms and gave a distance from the electron to the proton of ~1.4 Å. The ESR parameters obtained from the spectra are collected together in Table I. The g factors are close to the free-spin value and HFI are similar to those in adamantane, i.e., very small negative deviations from the values for gas-phase atoms.

Arene Substrates. Benzene. Copper. The ESR spectrum arising from deposition of ^{63}Cu into C_6H_6 is shown in Figure 3. It extends from ~100 G to just over ~5000 G and is similar in some respects to the spectra obtained by Kasai, McLeod, and Watanabe[10] for Cu atoms in argon containing low concentrations of ethylene and

---

(30) Trammell, G. T.; Zeldes, H.; Livingston, R. *Phys. Rev.* **1958**, *110*, 630–634.

(31) Ovenall, D. W.; Whiffen, D. H. *Mol. Phys.* **1961**, *4*, 135–144.

(32) Eachus, R. S.; Symons, M. C. R. *J. Chem. Soc. A* **1970**, 1329–1333.

(33) Bowman, M.; Kevan, L.; Schwartz, R. N. *Chem. Phys. Lett.* **1981**, *30*, 208.

(34) Narayana, M.; Li, A. S. W.; Kevan, L. *J. Phys. Chem.* **1981**, *85*, 132–133.

(35) Ozin, G. A. *J. Am. Chem. Soc.* **1980**, *102*, 3301–3303.

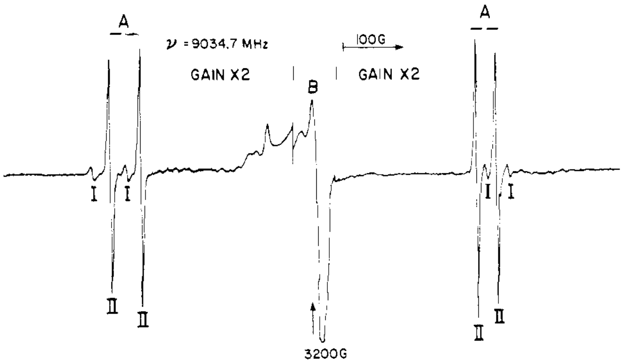

Figure 4. ESR spectrum of benzene containing ^{107}Ag and ^{109}Ag atoms at 77 K.

acetylene. It consists of two quartets labeled A(I) and A(II) with large Cu HFI and a complex multilined anisotropic central feature labeled B. If the quartets are treated as isotropic (see below), the following parameters are obtained: site I, A_{63} = 1547 G, g = 2.0036; site II, A_{63} = 1482 G, g = 2.0039. These parameters are similar to those reported by Zhitnikov and Kolesnikov[20] for Cu atoms stabilized in benzene at 77 K (A_{63} = 1547 G, g = 2.0044, A_{63} = 1480 G, g = 2.0050) and to the values for the ethylene and acetylene complexes of copper, $Cu(C_2H_4)$, and $Cu(C_2H_2)$.[10] We therefore assign these parameters to the mononobenzene complex of copper, $Cu(C_6H_6)$, in two magnetically distinct trapping sites.

Closer examination of the spectrum on an expanded scale shows that the lines corresponding to the $M_I = -^3/_2$ and $-^1/_2$ transitions are slightly but distinctly anisotropic, three principal features being evident for the highest field lines but only two for the lower field lines. The other transitions ($M_I = +^3/_2$ and $+^1/_2$) are essentially isotropic with $\Delta H_{pp} < 20$ G. Consequently, the complexes have orthorhombic symmetry with two almost identical axes, leading to almost uniaxial g and hyperfine coupling tensors. The following parameters were calculated for the two sites: site I ($^{63}Cu(C_6H_6)$): A_1 = 1545 G (4339 MHz), g_1 = 2.006; A_2 = 1548 G (4340 MHz), g_2 = 2.0035; A_3 = 1553 G (4344 MHz), g_3 = 1.999. site II ($^{63}Cu(C_6H_6)$): A_1 = 1478 G (4151 MHz), g_1 = 2.006; A_2 = 1481 G (4153 MHz), g_2 = 2.004; A_3 = 1488 G (4160 MHz), g_3 = 1.997.

The anisotropy in $Cu(C_6H_6)$ contrasts markedly with the isotropic spectra observed for Cu/adamantane and Cu/cyclohexane and indicates a bonding interaction between the copper atom and benzene.

The deviation of the g tensor from axial symmetry is small and may be caused by anisotropic terms arising from the orthorhombic nature of the matrix site. Treating the system as one having axial symmetry gives $g_\perp$ = 2.005 and $g_\parallel$ = 1.998. It is worth noting that $g_\perp > g_\parallel$ and $A_\perp \sim A_\parallel$, whereas $Cu(C_2H_4)$ and $Cu(C_2H_2)$ have $g_\parallel > g_\perp$ and $A_\parallel > A_\perp$.[10]

The ESR spectrum given by ^{63}Cu and C_6D_6 is the same as that for C_6H_6 apart from a small reduction (~25%) in line widths for $Cu(C_6D_6)$. The shape and width of the central feature are identical in C_6H_6 and C_6D_6, indicating that none of the lines are due to hyperfine interaction with the protons of benzene.

Almost identical spectra are observed for ^{63}Cu and $^{13}C_6H_6$ except for ~50% increase in the line width for $Cu(^{13}C_6H_6)$. If this increase is due to spin density in the p orbitals of the benzene carbon atoms a spin density of ~20% is indicated. The width of the multiplet spectrum at $g = 2$ (B) is unaffected by the change from $^{12}C_6H_6$ to $^{13}C_6H_6$, confirming that the species responsible for this absorption is not derived from benzene. The absence of any change, apart from an improvement in resolution, for the multiplet centered around $g \sim 2$ shows that Zhitnikov's assignment of these features to a free-radical species is incorrect.[18]

Silver. The ESR spectrum of Ag atoms codeposited with benzene, shown in Figure 4, consists of two main features labeled A and B. The central region (B) is a composite spectrum similar to that found for copper. The spectrum from Ag_3[36] is not resolved in this system almost certainly because of the large number of lines from the two isotopes of silver and line broadening from the protonated matrix.

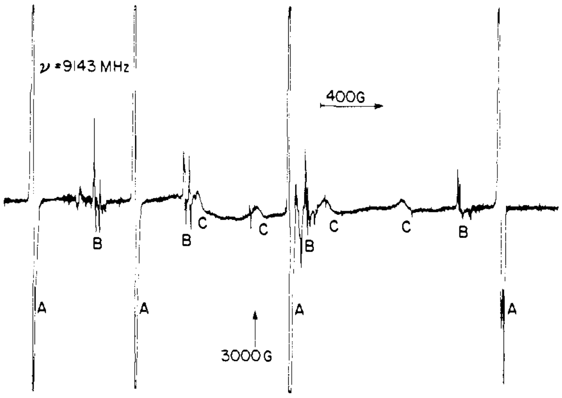

Figure 5. ESR spectrum of benzene containing ^{197}Au atoms at 77 K.

The transitions labeled A are the two doublets of doublets arising from the two silver isotopoes of spin $^1/_2$ in two trapping sites. The lines from site I are only a tenth as intense as those from site II and decay at a much faster rate on warming the sample. All the lines are isotropic and give the following parameters: site I: A_{109} = 700.6 G, g = 2.0006; A_{107} = 606.3 G, g = 2.0004; site II: A_{109} = 652 G, g = 2.0004, A_{107} = 565.4 G, g = 2.0009. These hyperfine coupling constants are 4% and 6% less than those in the corresponding two sites in adamantane and the g factors are significantly less than the free-spin value. They are assigned to the silver benzene complex $Ag(C_6H_6)$.

Each of the hyperfine lines from site II is accompanied by spin-flip satellites similar, but less well resolved, to those observed for Ag atoms in adamantane and cyclohexane.

The ESR spectrum from silver atoms deposited in C_6D_6 is similar to the spectrum shown in Figure 4 apart from a slight decrease in ΔH_{pp} for I and II, e.g., ΔH_{pp} for I decrease from 5.6 G to 3.4 G, and the absence of proton "spin-flip" satellite lines. Similarly, the use of $^{13}C_6H_6$ with silver atoms only produces a broadening of the lines (ΔH_{pp} for set I increasing to ~10 G). Both of these results indicate some unpaired spin population on the benzene molecule.

It is worth noting that the details of the spectra for silver are very sensitive to changes in experimental conditions such as the temperature and position of the furnace. This is especially true for the multitude of lines in the $g \sim 2$ region of the spectrum.

Gold. The ESR spectrum from gold atoms deposited with benzene (Figure 5) is a complex composite spectrum arising from gold–benzene complexes, gold clusters, and microcrystallites. There is one quartet (A) with a large Au HFI, indicating a single trapping site in this system. Treating the lines as isotropic gives the following ESR parameters: A_{Au} = 961 G g = 2.000, which, by analogy with Cu and Ag, we assign to $Au(C_6H_6)$. The HFI is 6% less than that of Au atoms in adamantane, indicating that the SOMO has largely s-orbital character. In this respect $Au(C_6H_6)$ is more like $Ag(C_6H_6)$ than $Cu(C_6H_6)$. Unlike $Ag(C_6H_6)$, however, the high-field line ($M_I = -^3/_2$) is unsymmetric and two principal features are apparent ($A_\parallel$ = 2707 MHz, $g_\parallel$ = 1.991; $A_\perp$ = 2687 MHz, $g_\perp$ = 2.0021). $Au(C_6H_6)$ is, therefore, like $Cu(C_6H_6)$ in that $g_\perp > g_\parallel$.

The species labeled B and C have Au HFI of 700 G and 400 G, respectively and are species that have not yet been positively identified.

Substituted Benzenes. Most of the substituted benzenes did not give matrices which could be transferred easily. In these cases cyclohexane was used as the trapping matrix, a ratio of cyclohexane to the substituted benzene of 10:1 being used.

Toluene. Reaction of copper atoms with toluene gives only an anisotropic spectrum in the region of $g = 2$ which is probably

---

(36) Howard, J. A.; Preston, K. F.; Mile, B. *J. Am. Chem. Soc.* **1981**, *103*, 6226.

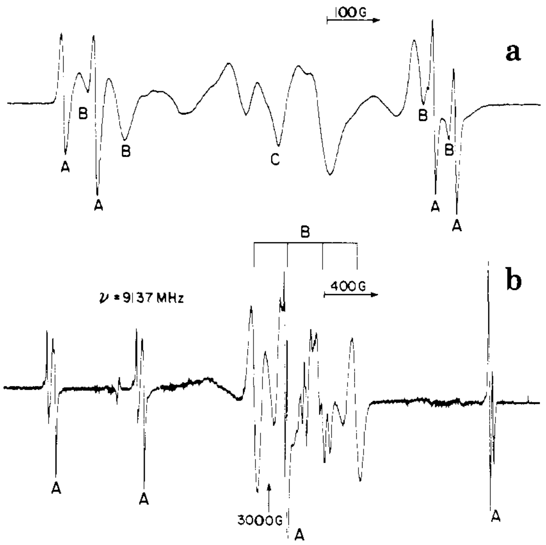

Figure 6. ESR spectra of cyclohexane containing (a) codeposited Ag atoms and cyanobenzene and (b) codeposited Au atoms and cyanobenzene.

associated with copper aggregates. There is no evidence for $Cu(C_6H_5CH_3)$ and isolated Cu atoms. Silver, on the other hand, reacts with toluene to give a complex spectrum which shows the presence of a silver species with a large Ag HFI, $A_{107} = 567.8$ G and $g = 2.0004$, parameters which are similar to those reported by Jezierska and Raynor[25] and Zhitnikov, Mel'nikov, and Orbeli[24] for Ag atoms in toluene.

Reaction of Au atoms with toluene in cyclohexane gives two quartets with the parameters $A_{Au} = 1069.4$ G, $g = 2.0029$, $A_{Au} = 1044.7$ G, $g = 2.0032$, which are identical with the values for Au in cyclohexane. In addition, there is a quartet of broad slightly anisotropic lines with $A_{Au} \sim 742$ G, $g \sim 1.91$, a third quartet with $A_{Au} \sim 240$ G, $g \sim 2.002$, and a broad anisotropic feature at the center of the spectrum. These latter species have not yet been identified although the central feature is almost certainly associated with Au microcrystallites.

Cyanobenzene. The ESR spectrum of silver atoms reacted with cyanobenzene in cyclohexane at 77 K (Figure 6a) is made up of transitions from at least three distinct species. The species labeled A has the ESR parameters $A_{109} = 711.9$ G, $g = 2.0023$, $A_{107} = 618.7$ G, $g = 2.0021$, values very close to the parameters for Ag in cyclohexane.

The species labeled B has very much broader lines ($\Delta H_{pp} \sim 30$ G) and ESR parameters $A_{109} = 649$ G, $g = 1.9996$, $A_{107} = 554.8$ G, $g = 2.0024$, values similar to those for $Ag(C_6H_6)$ in site II in benzene, and we conclude that this species is the silver–cyanobenzene complex $Ag(C_6H_5CN)$. This species is very unstable and decays rapidly even at 103 K.

The feature at the center of the spectrum partially resolves into a doublet of triplets at 103 K with a doublet spacing of ~100 G and a triplet spacing of ~23 G. We tentatively assign this spectrum to silver phenyl alkylidene aminyl $C_6H_5(Ag)C{=}\dot{N}$.

Reaction of Au atoms with cyanobenzene in cyclohexane gives the ESR spectrum shown in Figure 6b. The two quartets labeled A have the ESR parameters $A_{Au} = 1069.4$ G, $g = 2.0038$, $A_{Au} = 1044$ G, $g = 2.0030$, values which are identical with the parameters for Au atoms in two magnetically nonequivalent sites in cyclohexane.

The center feature labeled B is a quartet which we tentatively assign to $C_6H_5(Au)C{=}N$ with a quartet spacing of ~ 250 G.

Copper atoms react with cyanobenzene to give features at $g = 2$ which can only be assigned to clusters and microcrystallites; there is no evidence for the formation of $Cu(C_6H_5CN)$ or $C_6H_5(Cu)C{=}\dot{N}$.

Methoxybenzene. Silver and gold react with methoxybenzene in cyclohexane at 77 K to give two sets of lines with large HFI. The parameters for the silver species are $A_{109} = 706$ G, $g = 2.002$, $A_{107} = 612$ G, $g = 2.002$; $A_{109} = 678$ G, $g = 2.0004$, $A_{107} = 587$ G, $g = 2.0009$, and it appears that isolated Ag atoms and the complex $Ag(C_6H_5OMe)$ are formed in this system. The complex is, however, not very stable and disappears rapidly at 113 K. The ESR parameters for the Au species are identical with the values in cyclohexane and it would appear that a $Au(C_6H_5OMe)$ is not formed.

Table II. ESR Parameters for Complexes between Group 1B Metal Atoms and Benzene at 77 K

metal (M)	complex	*g* factor	A_M/MHz
^{63}Cu	$^{63}Cu(C_6H_6)$ site I	$g_1 = 2.006$ $g_2 = 2.005$ $g_3 = 1.999$	$A_1 = 4339$ $A_2 = 4340$ $A_3 = 4344$
^{63}Cu	$^{63}Cu(C_6H_6)$ site II	$g_1 = 2.006$ $g_2 = 2.004$ $g_3 = 1.997$	$A_1 = 4151$ $A_2 = 4153$ $A_3 = 4160$
^{107}Ag	$^{107}Ag(C_6H_6)$ site I	2.0004	1697.5 (606.3 G)
^{107}Ag	$^{107}Ag(C_6H_6)$ site II	2.0009	1579.4 (565.4 G)
^{197}Au	$^{197}Au(C_6H_6)$	2.0021 1.991	$A_\perp = 2687$ $A_\parallel = 2707$

Table III. ESR Parameters of Complexes of Ag and Au with Substituted Benzenes at 77 K

metal	complex	*g* tensor	A_M/G
	Toluene Complex		
^{107}Ag	$^{107}Ag(C_6H_5CH_3)$	2.0004	567.8
	Mesitylene Complexes		
^{107}Ag	$^{107}Ag(C_6H_3(CH_3)_3)$	2.0004	562.0
^{197}Au	$^{107}Au(C_6H_3(CH_3)_3)$	2.0005	963.0
	Cyanobenzene Complex		
^{107}Ag	$Ag(C_6H_5CN)$	2.0024	554.8
	Methoxybenzene Complex		
^{107}Ag	$Ag(C_6H_5OMe)$	2.0009	587

***o*-, *m*-, *p*-Xylenes and Mesitylene.** Only the multiplet of lines centered at $g \sim 2$ are observed in the spectrum of copper atoms deposited on these di- and trisubstituted benzenes. However, for silver and gold atoms complexes are seen with ESR parameters close to those for unsubstituted and monosubstituted benzenes except that the lines are much broader. The parameters for all the substituted benzenes are collected together in Table III.

Perfluorobenzene. Only anisotropic absorption lines at $g \sim 2$ are observed for group 1B metals with C_6F_6. The electron withdrawing fluorine would appear to destabilize metal atom–arene complexes in all cases.

Discussion

The ESR parameters of group 1B metal atoms trapped in inert hydrocarbons and of group 1B metal atom–monoarene complexes are collected in Tables I, II, and III. Stable arene complexes of zero valent group 1B metal atoms are unknown although labile complexes have been observed at 77 K but not characterized by Klabunde and Efner.[37] Molecular complexes of halogen molecules with benzene where benzene is the donor molecule are well-known.[38]

In the case of the stable bis-arene complexes such as $Cr(C_6H_6)_2$ and $W(C_6H_6)_2$ the eighteen-electron rule, to attain the configuration of krypton, is obeyed, while $M(C_6H_6)$, with their full d shells, have seventeen electrons. The full d shell will reduce back donation of electrons from the benzene to metal atom and decrease their stability. Nevertheless, we believe that the ESR spectra observed are due to genuine complexes and are not merely the result of metal atoms trapped by van der Waals forces in the arene matrix. Three features support this view: first, the 50% reduction

---

(37) Klabunde, K. J; Efner, H. F. *J. Fluorine Chem.* **1974** *4*, 114–116.

(38) See, for example, "Molecular Complexes"; Foster, R., Ed.; Crane Russack and Co. Inc.: New York, 1973.

Table IV. Percentage s-Orbital Contribution to the Semi-Occupied Orbital of $M(C_6H_6)$ Based on Calculated Values of A^a (A) and Experimental[b] Values of A_{iso} (B)

complex	A	B
$Cu(C_6H_6)$	69–72	72
$Ag(C_6H_6)$	86	95
$Au(C_6H_6)$	94	94

[a] From ref 39. [b] Smallest value in adamantane.

in the copper hyperfine coupling constant for $Cu(C_6H_6)$ together with the anisotropy of the spectrum suggests considerable electron reorganization and, therefore, bonding; secondly, the intense and characteristic colors of the complexes suggest bonding between the atom and benzene; thirdly, the much slower decay on warming of the $M(C_6H_6)$ spectra compared with the spectra of the corresponding atoms in adamantane and cyclohexane. The absence of copper complexes and the occurrence of silver and gold complexes of some substituted benzenes also argues for characteristic chemical bonding rather than unspecific physical trapping.

The Nature of the SOMO and the Bonding in $M(C_6H_6)$. The ESR parameters give direct information about the nature of the SOMO and indirect information about the nature of the bonding in these arene complexes. Let us consider first the values of the hyperfine coupling tensors. Treating the tensors for $Cu(C_6H_6)$ and $Au(C_6H_6)$, as axially symmetric ($Ag(C_6H_6)$ is totally symmetric), the isotropic and dipolar components A_{iso} and A_{dip} can be determined from the experimental $A_{\parallel}$ and $A_{\perp}$ values using the relationships $A_{\parallel} = A_{iso} + 2A_{dip}$ and $A_{\perp} = A_{iso} - A_{dip}$. The values obtained are as follows: $Cu(C_6H_6)$ (site I): $A_{iso}(^{63}Cu) = 4341$ MHz, $A_{dip}(^{63}Cu) = 1.5$ MHz; (site II): $A_{iso}(^{63}Cu) = 4154$ MHz, $A_{dip}(^{63}Cu) = 3$ MHz. $Ag(C_6H_6)$ (site I): $A_{iso}(^{107}Ag) = 1697.5$ MHz, $A_{dip}(^{107}Ag) = 0$; (site II): $A_{iso}(^{107}Ag) = 1597$ MHz, $A_{dip}(^{107}Ag) = 0$. $Au(C_6H_6)$: $A_{iso}(^{197}Au) \sim 2694$ MHz, $A_{dip}(^{197}Au) \sim 7$ MHz.

The percentage s character in the SOMO can be estimated from A_{iso} and the calculated value of the hyperfine interaction for unit spin density in an s orbital (A).[39] Alternatively, the experimentally observed values of A_{iso} in the gas phase, in rare gas matrices, and in inert hydrocarbon matrices such as adamantane and cyclohexane can be used. The values in adamantane and cyclohexane are probably more suitable for our work because they compensate, to some extent, for the increase in A_{iso} which arises from overlap and repulsive effects[28,29] with matrix molecules. The percentage s-orbital contribution to the SOMO based on A^{39} and the smallest A_{iso} in adamantane are given in Table IV. Clearly there is a large percentage of s character in the SOMO for $M(C_6H_6)$. The values for $Cu(C_6H_6)$ and $Ag(C_6H_6)$ are very close to those for $Cu(C_2H_2)$, $Cu(C_2H_4)$, $Ag(C_2H_2)$, and $Ag(C_2H_4)$.[10] There is no information available for $Au(C_2H_2)$ and $Au(C_2H_4)$.

The values of A_{dip} for $Cu(C_6H_6)$ and $Au(C_6H_6)$ are small, the value for $Cu(C_6H_6)$ being about $^1/_{10}A_{dip}$ for $Cu(C_2H_2)$ and $Cu(C_2H_4)$.[10] This suggests that if the SOMO for $Cu(C_6H_6)$ consists of 4s and 4p orbitals it has <4% 4p character and that the total unpaired spin population ($\rho_{4s} + \rho_{4p}$) is <74%. The atomic parameter for unit spin density in a 6p orbital of Au can be calculated to be 21.3 MHz from the fine structure spacing of the atomic spectrum of Au in the $^2P(5d^{10}6p^1)$ state.[40–42] This suggests that $\rho_{6p} \sim 0.33$ for $Au(C_6H_6)$ giving $\rho_{6s} + \rho_{6p} \sim 1.3$. Alternatively, if the SOMO consists only of s and d orbitals, ρ_{4d} for $Cu(C_6H_6)$ < 0.009 and ρ_{6d} for $Au(C_6H_6) \sim 0.18$,[39] giving total unpaired spin populations of 0.7 and 1.12. It is worth noting that the positive sign of $g_{\perp} - g_{\parallel}$ for $Cu(C_6H_6)$ suggests a larger d contribution to the SOMO than occurs for $Cu(C_2H_2)$ and $Cu(C_2H_4)$ which have negative values of $g_{\perp} - g_{\parallel}$.

The isotropic hyperfine coupling tensor of the silver complexes indicates very little contribution from p and d orbitals, although it should be noted that the atomic parameters 2P/5 (21.6 MHz) and 2P/7 (15.4 MHz) are small for ^{107}Ag 5p.[39–42] The g tensors are also isotropic but have negative shifts relative to the free spin value and the values in neon,[26] adamantane, and cyclohexane. An isotropic g tensor with a similar negative shift was observed for $Ag(C_2H_2)$, $Ag(C_2H_4)$,[10] and Ag atoms trapped in Ar, K, and Xe.[26] This perhaps implies that Ag atoms are not just trapped in arene matrices but that bonding or orbital overlap occurs and that there must be some p and/or d orbital contribution to the SOMO.

We conclude that the SOMO in the three benzene complexes studied have the following forms with less than 10% contribution from the benzene orbitals.

$$Cu(C_6H_6)\ \Phi = \sqrt{0.7}\phi(s) + \sqrt{(0.3 - x)}\phi(p) + \sqrt{x}\phi(d)$$

$$Ag(C_6H_6)\ \Phi = \phi(s)$$

$$Au(C_6H_6)\ \Phi = \sqrt{0.95}\phi(s) + \sqrt{(0.05 - x)}\phi(p) + \sqrt{x}(\phi)(d)$$

Kasai, McLeod, and Watanabe have suggested that the almost pure s nature of the SOMO for $Ag(C_2H_4)$ and $Ag(C_2H_2)$ indicates a pseudo complex bonded only by van der Waals interactions.[10] However, the nature of the SOMO may not provide a good basis for discussing the relative stability of the complexes since it can be a nonbonding or even an antibonding orbital. In fact, we find experimentally that $Ag(C_6H_6)$ is more stable than $Cu(C_6H_6)$ in that it decays more slowly ($\sim ^1/_{10}$) and its preparation is much less susceptibility to changes in experimental conditions.

The two most likely structures for $M(C_6H_6)$ are (I) a structure with the metal atom lying along the sixfold axis of the benzene molecule with bonding interactions between the π orbitals of the benzene ring and the s, p, and d orbitals of the metal atom, and (II) a structure with the metal atom interacting with only one localized C=C bond of the benzene ring, i.e., isostructural with $Al(C_6H_6)^{43}$ and of similar structure to the crystalline complexes $(C_6H_6)CuAlCl_4^{44}$ and $(C_6H_6)AgClO_4^{45}$ which have the metals ion Cu(I) and Ag(I) located directly above one C=C bond of the benzene ring. The ESR parameters clearly rule out metal-substituted cyclohexadienyls and $M^+(C_6H_5)^-$. The ESR spectrum of $Al(C_6H_6)^{43}$ does, however, indicate a small aluminum hyperfine interaction of ~20 G and hyperfine interactions with two equivalent protons of ~10 G, whereas $M(C_6H_6)$ have large M atom HFI and unresolved H HFI. $Al(C_6H_6)$ and $M(C_6H_6)$ must, therefore, have different structures and $M(C_6H_6)$ probably prefer structure I. It should also be noted that the interactions in $(C_6H_6)CuAlCl_4$ and $(C_6H_6)AgClO_4$ are primarily ionic and may lead to unusual structures as evidenced by the fact that the metal ion is asymmetrically placed between the two carbon atoms.

This assignment is supported by an INDO/S calculation on $Cu(C_6H_6)$ which indicates that the *hexahapto* complex is more stable than the *dihapto* complex. This calculation places the unpaired electron in the $6a_1$ orbital which has ~80% 4s and ~20% $4p_z$ orbital contributions from the copper atom, in a lobe pointing away from the benzene ring, with very little contribution from benzene orbitals. This is similar to Kasai, McLeod, and Watanabe's description of the SOMO for $Cu(C_2H_2)$ and $Cu(C_2H_4)$.[10] It is, however puzzling, that the ESR spectra of $Cu(C_2H_2)$, $Cu(C_2H_4)$, and $Cu(C_6H_6)$ indicate that these complexes have similar unpaired s-spin populations but that the arene complex has a much smaller unpaired p-spin population. This may be associated with the fact that $g_{\parallel} - g_{\perp}$ for $Cu(C_6H_6)$ and the other two complexes have different signs.

Bonding in $Cu(C_6H_6)$, from INDO calculations, appears to be largely the result of stabilizing interactions between π orbitals of benzene and hybridized the d_{yz}–p_y and d_{xz}–p_x orbitals of the copper atom. The MO description has ~80% benzene and ~20% metal atom orbital contributions. This suggests that there is a donation of charge from the benzene π orbitals to the empty 4p

---

[39] Morton, J. R.; Preston, K. F. *J. Magn. Res.* **1978** *30*, 577–582.

[40] Moore, C. E. *Natl. Bur. Stand. (U.S.) Circ.* **1952**, *No. 467*; **1958**; 3.

[41] Townes, C. H.; Schawlow, A. L. "Microwave Spectroscopy"; McGraw-Hill: New York, 1955; Chapter 5.

[42] Barnes, R. G.; Smith, W. V. *Phys. Rev.* **1954**; *93*, 95–98.

[43] Kasai, P. H.; McLeod, D., Jr. *J. Am. Chem. Soc.* **1979**, *101*, 5860–5862.

[44] Turner, R. W.; Amma, E. L. *J. Am. Chem. Soc.* **1966**, *88*, 1877–1882.

[45] Smith, H. G.; Rundle, R. E. *J. Am. Chem. Soc.* **1958**, *80*, 5075–5080.

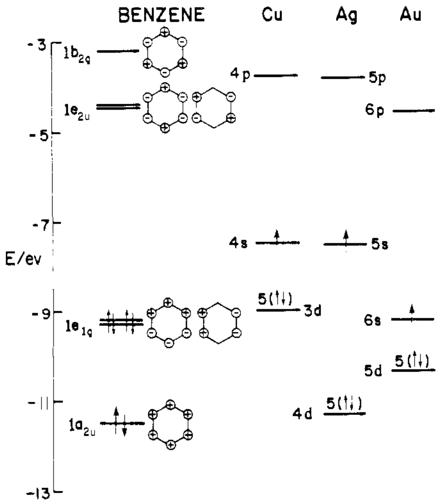

Figure 7. Interaction diagram for Cu, Ag, and Au atoms and benzene.

orbitals and a back donation of charge from the metal 3d orbitals to the benzene π orbitals. There does not appear to be a bonding interaction between the benzene π^* orbitals and the copper d orbitals as suggested by Kasai, McLeod, and Watanabe[10] for $Cu(C_2H_2)$ and $Cu(C_2H_4)$. Our description of the bonding is similar to the one that emerges from McIntosh, Ozin, and Messmers'[12] SCF-Xα-SW calculations on $Cu(C_2H_2)$ and $Cu(C_2H_4)$. The INDO calculation does, however, give more p-orbital contribution than is apparent from SCF-Xα-SW calculations.

The apparent difference in structure between $Al(C_6H_6)$ and $Cu(C_6H_6)$ is probably because of the size of the valence p orbitals of Al. The more compact p orbital cannot effectively interact with the π orbitals of benzene in the sixfold symmetry.

Owing to limitations in the INDO/S program, we cannot perform calculations on $Ag(C_6H_6)$ and $Au(C_6H_6)$. The ESR parameters, viz., high metal HFI and unresolved H HFI, do, however, suggest a structure with sixfold symmetry.

An energy correlation diagram for group 1B metal atoms and benzene is shown in Figure 7 and it is apparent that the $3d_{xz}$ and $3d_{yz}$ orbitals of Cu are close in energy to the benzene $1e_{1g}$ orbitals and of the correct symmetry for interaction to take place while the silver $4d_{z^2}$ orbital is closer and of the correct symmetry to interact with the $1a_{2u}$ orbital. The increased stability of $Ag(C_6H_6)$ may be associated with more favorable overlap in the latter case.

Substituting benzene with electron donating and withdrawing groups, such as CH_3, CH_3O, CN, and F, destabilizes copper-arene complexes but has very little influence on the stability and ESR parameters of silver and gold arene complexes. This may be associated with the fact that ring substitution has a larger effect on the energy of the $1e_{1g}$ orbitals than on the lower $1a_{2u}$ orbitals.[46-48] Two extreme samples are a lowering of the $1e_{1g}$ levels by 0.6 eV in cyanobenzene and a lifting by 0.86 eV in anisole while the $1a_{2u}$ level is shifted in the same directions by only 0.3 eV. This would appear to support our description of the bonding in group 1B metal atom-benzene complexes.

Ending on a cautionary note, it is worth adding that additional features associated with the arrangement of matrix molecules on the nonbenzene side of the metal atom may also influence the stability of these labile complexes and that such interactions may also change with substitution of the benzene. However, it is unlikely that the marked difference between copper, silver, and gold atoms can be attributed solely to such differences in the trapping sites.

Acknowledgment. We thank Mr. D. Malenson and Dr. D. B. Clegg (Liverpool Polytechnic) for help with the high-temperature furnace and the computer iteration program, respectively. In addition, we thank Mr. J. H. B. Chenier for assistance with the experimental work and Drs. K. F. Preston, J. R. Morton, R. Sutcliffe, and J. S. Tse for many helpful discussions. The award of a SERC (CASE) studentship to A.J.B. is also gratefully acknowledged as is financial assistance and equipment from Shell Research Ltd.

Registry No. Cu, 7440-50-8; Ag, 7440-22-4; Au, 7440-57-5; $Cu(C_6H_6)$, 85371-08-0; $Cu(C_6D_6)$, 85371-09-1; $Cu(^{13}C_6H_6)$, 85389-81-7; $Ag(C_6H_6)$, 85371-10-4; $Ag(C_6D_6)$, 85371-11-5; $Ag(^{13}C_6H_6)$, 85389-82-8; $Au(C_6H_6)$, 85371-12-6; $Ag(C_6H_5CH_3)$, 85371-13-7; $Ag(C_6H_3(CH_3)_3)$, 85371-14-8; $Au(C_6H_3(CH_3)_3)$, 85371-15-9; $Ag(C_6H_5CN)$, 85371-16-0; $Ag(C_6H_5OMe)$, 85371-17-1; adamantane, 281-23-2; cyclohexane, 110-82-7; benzene, 71-43-2; toluene, 108-88-3; cyanobenzene, 100-47-0; methoxybenzene, 100-66-3; *o*-xylene, 95-47-6; *m*-xylene, 108-38-3; *p*-xylene, 106-42-3; mesitylene, 108-67-8; perfluorobenzene, 932-56-3.

---

(46) "The Photoelectron Spectroscopy of Molecules"; Faraday *Discuss. Chem. Soc.* **1972**, *54*.

(47) Baker, A. D.; May, D. P.; Turner, D. W. *J. Chem. Soc. B* **1968**, 22-34.

(48) Koopmans, T. *Physica*, **1933**, *1*, 104-113.